Published in final edited form as:

Mov Disord. 2016 December ; 31(12): 1846–1853. doi:10.1002/mds.26732.

Stop-related subthalamic beta activity indexes global motor suppression in Parkinson's Disease

Jan R. Wessel, Ph.D.[1,2,3,*], **Ayda Ghahremani, MASc.**[4,5,*], **Kaviraja Udupa, M.D., Ph.D.**[4,6], **Utpal Saha**[4,6], **Suneil K. Kalia, M.D., Ph.D.**[4,7], **Mojgan Hodaie, M.D.**[4,7], **Andres M. Lozano, M.D., Ph.D.**[4,7], **Adam R. Aron, Ph.D.**[3], and **Robert Chen, MBBChir.**[4,6]

[1]Department of Psychological and Brain Sciences, University of Iowa, Iowa City, IA 52242, USA

[2]Department of Neurology, University of Iowa, Iowa City, IA 52242, USA

[3]Department of Psychology, University of California San Diego, La Jolla, CA 92093, USA

[4]Toronto Western Research Institute, Toronto, ON, CA

[5]Institute of Medical Science, University of Toronto, Toronto, ON, CA

[6]Division of Neurology, Department of Medicine, University of Toronto, Toronto, ON, CA

[7]Division of Neurosurgery, Department of Surgery, University of Toronto, Toronto, ON, CA

Abstract

Background—Rapid action-stopping leads to global motor suppression. This is shown by studies using Transcranial Magnetic Stimulation to measure corticospinal excitability of task-unrelated effectors, e.g., from the hand during speech-stopping. We hypothesize this global suppression relates to the subthalamic nucleus of the basal ganglia. Several STN local field potential studies in Parkinson's patients have shown increased ß-band power during successful stopping. Here, we aimed to test whether this STN ß-band activity indexes global motor suppression measured by transcranial magnetic stimulation.

Corresponding author address Jan R. Wessel, Ph.D., Department of Psychological and Brain Sciences, Department of Neurology, University of Iowa, E114 Seashore Hall, Iowa City, IA 52242, Phone: 319 335 2486, jan-wessel@uiowa.edu.
*Equal contribution

AUTHOR ROLES

JRW, ARA, RC designed research. JRW programmed the experiment. AG, KU, US, SKK, MH, AML, RC performed research. JRW analyzed the data. JRW drafted the manuscript. JRW, ARA, RC edited the manuscript. All authors approved the final version of the manuscript.

FINANCIAL DISCLOSURES

JRW: None.
AG: None.
KU: None.
US: None.
SKK: None.
MH: None.
AML: None.
ARA: None.
RC: Consultant: Allergan and Merz, Research grant: Medtronic Inc., Merz

The authors have no financial conflict of interest.

Methods—We studied nine medicated PD patients (age: 47 – 67y, mean: 55.8; 3 female) who were implanted with STN-DBS electrodes. Participants performed a vocal stop-signal task (i.e., they had to occasionally stop a vocal response) while we simultaneously recorded local field potentials from right STN and delivered transcranial magnetic stimulation to primary motor cortex to measure corticospinal excitability from a task-unrelated hand muscle (first dorsal interosseous).

Results—Replicating prior results, STN ß-band power was increased ($p < .005$) and corticospinal excitability was reduced ($p = .024$) (global motor suppression) during successful stopping. As hypothesized, such global motor suppression was greater for successful stop-trials with higher STN ß-power (median-split: $p = .043$), which was further evident in a negative correlation between single-trial STN ß-power and corticospinal excitability (mean $r = -.176$, $p = .011$).

Conclusion—These findings link stopping-related global motor suppression to STN ß-band activity through simultaneous recordings of STN and corticospinal excitability. The results support models of basal ganglia that propose the STN has broad motor suppressive effects.

Keywords

Response inhibition; Subthalamic Nucleus; Beta-Band; Motor evoked potentials; Corticospinal Excitability

INTRODUCTION

Quickly stopping an initiated movement is a well-studied control process. It is implemented by a fronto-basal ganglia network including the pre-supplementary motor area, the right inferior frontal cortex, and the subthalamic nucleus (STN) of the basal ganglia (for reviews, see [1, 2-4]). An interesting feature of rapid action-stopping is its global motor effects, evident from studies that measure corticospinal excitability (CSE) using single-pulse TMS of primary motor cortex. During rapid action-stopping, CSE is reduced not only in the targeted motor effector, but also in task-unrelated motor effectors, even at rest. For example, stopping the hand leads to CSE reductions in the leg [5, 6], and stopping eye-movements or speech leads to reduced CSE of the hand [7, 8]. The neural mechanism underlying stopping-related global motor suppression is currently unknown, but one possibility is that it relates to the STN. STN activity is increased during action-stopping in single unit recordings from rodents, monkeys and humans [9-11], in fMRI [12, 13], and in LFP recordings from PD patients with implanted STN electrodes (especially in the ß frequency band [11, 14-16]; 12-24Hz[17]). Lesions to the STN in rodents [18] and humans [19] also adversely affect action-stopping. Anatomical tracing studies suggest that the STN has a wide projection to the basal ganglia output nuclei [20], leading to proposals that it could issue a broad, non-selective stop command [21-23]. Here, we tested whether global suppression of CSE (measured by TMS) relates to STN activity (measured by intracranial depth electrodes) during action-stopping.

We studied nine patients with implanted STN electrodes for the treatment of PD. They performed a vocal version of the stop-signal task (SST). We recorded LFPs from the STN, while simultaneously delivering TMS over the hand area of the primary cortex to measure global motor suppression. Based on the findings presented above, we expected that successful stopping would be accompanied by both increased STN beta-band activity [15] and

reduced CSE from the task-unrelated hand [7]. Importantly, we predicted that greater single-trial STN beta-band activity during successful stopping would relate to greater CSE reduction: i.e., greater beta-band activity immediately before the CSE probe should correspond to greater global motor suppression.

MATERIALS AND METHODS

Participants

Nine right-handed PD patients undergoing STN electrode (Medtronic model 3387) implantation for deep brain stimulation (age: 47 – 67y, mean: 55.8; 3 female) took part in the experiment. Patients were tested on their usual therapeutic medications to best normalize motor and cognitive abilities. Patients were tested 1-4 days after surgery, when the leads remained externalized, prior to connection to the pulse generator. All patients provided written informed consent and the protocol was approved by the University Health Network (Toronto) Research Ethics Board.

Paradigm

We used a vocal version of the SST (Figure 1). Each trial began with a fixation cross (1,000ms), followed by a go-stimulus (the letters T or K). Participants were instructed to respond as fast as possible by speaking the letter into a microphone (1,500ms deadline) unless a stop-signal appeared (the letter turned red). This happened pseudorandomly, with a probability of 33%. The delay between stop-signal and go-stimulus (stop-signal delay, SSD) was initially set to 200ms and then automatically adjusted to achieve a probability of successful stopping [p(stop)] of .5 (SSD was increased by 50ms after successful and decreased by 50ms after failed stopping). Participants were instructed that successful stopping and quick responding were equally important. After response emission, the letter disappeared and the inter-trial interval began (overall trial duration: 3,500ms).

Materials

Stimuli were presented on an Apple MacBook running MATLAB and Psychtoolbox 3 [24]. Responses were recorded using a Logitech USB microphone.

Procedure

First, the microphone was manually calibrated to detect the voice onset of each participant (see [25]). Then, participants performed 132 trials (4 blocks) of the SST. During this part, only LFPs were recorded (no TMS stimulation was applied). Finally, participants performed another 300 trials (6 blocks) of the SST, during which LFPs were recorded and TMS was simultaneously delivered (along with concurrent electromyography) to measure CSE.

TMS

TMS was performed with a 6 cm figure-of-eight coil, using two Magstim 200 stimulators and a Bistim module (Magstim Company, Dyfed, UK), delivering stimuli by alternating between stimulators. The area that elicited the best motor response in the right FDI muscle was established over left M1 with the coil held about 45 degrees to the mid-sagittal line

(approximately perpendicular to the central sulcus). The direction of the induced current was from posterior to anterior and was optimal to activate the corticospinal neurons transynaptically. The optimal position was marked on the scalp to ensure identical placement of the coil throughout the experiment. A suprathreshold pulse (minimum stimulus intensity that produced > 1mV motor-evoked potentials [MEPs] in 5/10 trials) was used throughout the experiment. TMS was applied at 110% of the threshold (Mean intensity=56% of maximum output; min=44%, max=70%).

Based on our earlier paper on global motor suppression during the vocal SST [7], we time-locked TMS pulses to an online estimate of go-trial reaction time (GoRT). Specifically, GoRT was initially quantified based on the LFP-only phase, and then updated in the simultaneous LFP-TMS phase through a moving average of the previous 30 go-trials. Stimulation was delivered at GoRT-100ms, which corresponds to the time point of maximal motor suppression[7]. Based on this calculation, the stimulation occurred on average at 587ms (go-trials), 572ms (successful stop-trials), and 575ms (failed-stop trials) post-go-stimulus (rmANOVA revealed no systematic differences between conditions, $p > .16$). On 30 random go-trials, stimulation was applied in the inter-trial interval (500ms after the response deadline) instead of at GoRT-100ms. These trials served as a baseline for normalization. On trials following these baseline trials, no stimulation was delivered to allow the stimulators to recharge.

LFP and electromyography (EMG) recording

LFP was recorded from all four contacts of the bilateral STN depth-electrodes using the externalized lead. We focused on the right STN because an fMRI study showed greater activity in right STN during action-stopping[12], which is confirmed by a meta-analytic search of “response inhibition” on neurosynth.org. However, we also present the results from the left electrodes. The signal was amplified using SynAmp amplifiers and digitized using a Neuroscan system (Neuroscan Laboratories, El Paso, Texas, USA, gain: 2500). LFP signals were sampled at 2,500Hz and band-pass filtered between 1-100Hz. EMG was recorded via adhesive electrodes (9 mm diameter Ag–AgCl electrodes; active electrode placed over the muscle belly, reference electrode over the metacarpophalangeal joint of the index finger) from the right first digital interosseus (FDI) muscle and amplified (sampling rate: 2,500Hz; band-pass filter: 30-500Hz).

Behavioral analysis

We quantified GoRT (voice-onset on correct go-trials), RT on failed-stop trials (FsRT, voice-onset on trials with stop-signals), mean SSD, and stop-signal reaction time (SSRT). GoRT was compared to FsRT using a paired-samples t-test to ensure that SSRT calculations using the mean method [26] were appropriate. SSRT was calculated by subtracting the average stop-signal delay (SSD) from the average GoRT.

STN-LFP beta difference validation

We analyzed the unimodal LFP data to ensure that the previously reported STN beta-power increase for successful vs. failed stopping [15] was also present in our sample. Raw data from the LFP-only phase were imported into MATLAB, re-referenced to adjacent-neighbor

dipolar references (contact 0 – contact 1, contact 1 – contact 2, and so forth), and resampled to 500Hz. After visual inspection and artifact rejection, event-related spectral perturbation (ERSP) was quantified using the absolute of the Hilbert transformation for 13 individual frequencies spanning the beta-band (12 to 24Hz[17], frequency window: +/-0.5Hz). The ERSP was quantified in units of percent change from baseline (-500ms to 0ms before the go-signal) and averaged for successful and failed stop-trials separately, over a time-period of 1000ms following the stop-signal. Differences in beta-band power between the two trial types were tested using sample-to-sample Wilcoxon's signed rank tests at a two-sided p-value of p = .05, which was corrected to p = .004 to correct for the comparison of multiple frequencies (Bonferroni correction for 13 individual frequencies). The non-parametric Wilcoxon test was used because neural activity is likely non-normally distributed, and our sample size was limited to N=9.

Global CSE suppression validation

We analyzed the CSE data to ensure that the previously reported CSE reduction for the FDI muscle during vocal stopping[7] was also present in our patient sample. CSE was quantified from the MEP in the EMG trace. After import into MATLAB, EMG data were notch filtered at 60Hz. MEP amplitudes were then quantified using a peak-to-peak measurement in the time period 50ms after the TMS stimulus. The accuracy of the automated quantification was checked by visual inspection of each individual trial (trial-type was blinded). Trials with visible artifacts and trials in which the automated algorithm failed were rejected from subsequent analysis, as were trials in which TMS occurred after response emission (this could happen because of the probabilistic nature of the GoRT-forecast, and trial-by-trial variability in RT). MEPs were normalized by the average MEP on the 30 baseline trials to account for inter-individual variability. MEPs were averaged separately for each trial type (go, successful-stop, failed-stop) and compared using repeated-measures ANOVA (two-sided p = .05). Furthermore, we calculated planned contrasts of successful-stop < go and successful-stop < failed-stop, (p = .05, two-sided).

Simultaneous LFP-TMS analysis

We tested our main hypothesis based on the simultaneous LFP-TMS data. For each stop-trial with a valid MEP in the simultaneous LFP-TMS phase, beta-band power was quantified immediately before the TMS pulse. This time period (168ms – 0ms before the TMS stimulus, which fits 2 cycles at the lower frequency bound of 12Hz) was transformed into time-frequency space using a hamming-windowed Fast-Fourier Transformation (FFT). Based on the mean TMS stimulation-time on successful stop-trials (572ms post-go-stimulus), this time period ranged from 404ms – 572ms after go-signal onset (which corresponds to 41ms – 209ms post-stop-signal onset). FFT estimates for the beta-band were averaged, and the FFT average for a baseline period spanning 168ms before go-stimulus onset was subtracted. To select the bipolar STN channel for the LFP-MEP analysis (from all available dipolar montages), we quantified the beta-band difference between all stop and go-trials for each dipolar channel. We then selected the channel with the biggest difference between these two trial types. This difference contrast served as a functional localizer based on prior literature [15]. This does not bias the analysis towards finding a relation with the MEP, and the subsequent LFP-MEP analysis was done on successful stop-trials only.

Furthermore, selecting a different subset of channels (based on the maximal beta-difference between *successful and failed stop trials*) did not change the pattern of results.

Outliers in the single-trial LFP and MEP data were diagnosed using Grubbs' test for outliers (p = .05) and removed from this single-trial analysis. Each successful stop-trial was then classified as either high or low in beta power, based on a median split within each subject. Successful-stop trial MEP amplitudes were then averaged for high and low beta trials separately, and tested against each other using a paired samples t-test (p = .05), which tested our hypothesis of greater MEP suppression on high-beta trials.

We used the median split method because of the high-levels of noise inherent in single-trial MEP data. However, we also tested the relationship between MEP suppression and beta power on a trial-to-trial level within subjects. To this end, instead of median-splitting single-trial MEP amplitudes based on beta-power, we correlated single-trial beta-power and MEP amplitudes on successful stop-trials directly within each subject using the Pearson correlation coefficient. We then tested these coefficients for significance on the group-level using a truth-label switching monte-carlo simulation (10,000 iterations). In each iteration, we randomly shuffled the successful stop-trial LFP and MEP ampltiudes within each subject and generated a group-level correlation based on the shuffled trials. The group-level (average) correlation for each iteration was then computed and compared to the actual group-level mean correlation for the actual data. The p-value is then derived by comparing how many of the 10,000 group-level correlation coefficients generated based on random trials were more (or just as) positive / negative as the original coefficient. If fewer than 500 coefficients are as extreme as (or more extreme than) the original correlation coefficient, the test is significant at p = .05.

RESULTS

Behavior

Behavioral results are summarized in Table 1. In the LFP-only phase, GoRT was greater than FsRT for all nine participants ($t(8) = 3.8$, $p = .005$, $d = 1.18$) as expected based on the race model for the stop signal task. In the simultaneous LFP-TMS phase, GoRT was again greater than FsRT for all nine participants ($t(8) = 8.1$, $p < .001$, $d = 1.2$). None of the behavioral measures differed between the LFP-only phase and the simultaneous LFP-TMS phase (cf. Table 1), showing that the application of TMS did not significantly influence stopping behavior.

Validation: STN-LFP beta difference (LFP-only)

Figure 2A shows the group-level ERSP difference between successful and failed stop-trials at the dipolar right STN contacts selected for the simultaneous LFP-MEP analysis (the contacts for these analyses were independently selected based on the simultaneous dataset). Figure 2B shows the power spectra for these contacts. Beta-power amplitude was increased for successful vs. failed stop-trials right toward the end of SSRT (which is where inhibition should be maximal according to computational models of the stop-signal task[27]). The difference was significant at p = .004 (two-sided) at 378 – 416ms post-stop signal (Figure

2A, black outline). No other frequency band showed significant differences between the two trial types at the corrected significance threshold. The left STN electrode also showed increased beta-band activity in a similar time-range, yet this did not reach significance at the corrected threshold of p = .004.

Validation: Global CSE suppression

Figure 3A shows the differences in MEP amplitudes based on trial condition. MEP amplitudes were significantly different between trial types ($F(2/16) = 5.4$, $p = .016$, $\eta^2 = 0.4$). In line with prior studies, successful stop-trials showed reduced MEP amplitudes compared to both go-trials ($t(8) = 2.8$, $p = .023$, $d = 1.1$) and failed-stop trials ($t(8) = 2.78$, $p = .024$, $d = 1.1$).

Main hypothesis: Simultaneous LFP-MEP

In line with our hypothesis, MEP amplitudes on successful stop-trials were significantly smaller on trials with large STN beta-amplitudes compared to trials with small beta-amplitudes ($t(8) = 2.4$, $p = .043$, $d = 1.25$, Figure 3B). Figure 4 shows the individual participants' TMS data. All but one participant showed numerically reduced MEPs on successful stop-trials compared to go trials, and all but two participants showed numerically greater suppression on successful stop-trials with high-beta compared to low-beta (one was the aforementioned participant who showed no suppressed overall MEP). Just like for the LFP-only results, left STN electrodes showed the same numerical pattern (greater MEP suppression for high-beta trials) as right STN electrodes, yet like the LFP-only results, this did not reach significance at a two-sided p of = .05 ($t(8) = 1.16$, $p = .28$, $d = .6$).

The result of the median-split analysis for the right STN was further corroborated by the group-level correlation between single-trial beta-power and MEP amplitude on successful stop-trials. The mean correlation coefficient was -.176 (sem: .08), meaning that higher beta-power on individual successful stop-trials was accompanied by stronger CSE suppression (smaller MEP). Compared to the monte-carlo distribution, this group-level correlation was significant at $p = .011$.

To test whether this result was specific to action-stopping or whether increased beta is merely a marker of an akinetic state that is also indexed by reduced CSE, we repeated the analysis for go-trials. For this, we split go-trial MEP amplitudes by beta-power in the 168ms time-window preceding the TMS pulse. Here, we did not find the same relationship ($p > 0.46$). In fact, go-trials with large beta-amplitudes had numerically larger MEPs than go-trials with small beta-amplitudes. Thus, the relation between increased beta and lower CSE was specific to successful stop trials. This suggests that increased beta is not merely a marker of an akinetic state, but a functional marker of a process elicited specifically during successful stopping.

DISCUSSION

While participants performed a vocal stop-signal task, we recorded LFPs from the STN and simultaneously delivered TMS over the hand area of M1. We replicated studies showing increased beta-band STN power for successful vs. failed stop trials [11, 14-16], and also studies

showing that action-stopping reduces CSE in task-irrelevant motor effectors [5-8]. Most importantly, our main analysis showed that global motor suppression on successful stop-trials is directly related to increased right-lateral beta-band STN activity. These results firmly establish increased STN beta-band activity as a signature of response inhibition in humans, and go further by showing that STN activity is related to the 'global' nature of the suppression.

Our central finding linking global motor suppression on successful stop-trials to STN activity is consistent with influential models of the basal ganglia. Based on some anatomical evidence for divergent projections from the STN to the output nuclei of the basal ganglia (globus pallidus and substantia nigra pars reticulata, [20, 28]), these models propose that a cortico-subthalamic 'hyperdirect' pathway inhibits large areas of the thalamus and cerebral cortex (albeit as part of movement initiation and not rapid stopping, [22, 23]). Related to this concept, it has been proposed that the STN implements a global 'NoGo' signal during decision conflict to momentarily withhold responding or "hold-your-horses", [29]. Our findings suggest that CSE reductions from task-irrelevant effectors and STN beta-band power are indeed markers of such global suppression. This is relevant for many studies that have either shown STN activity during decision (and other) conflict [30-32], movement selection [33], switching [34], or post-error slowing [35, 36].

Our study shows a correlation between STN activity and global suppression. We are mindful that a correlation between two variables (STN activity and global CSE suppression) does not exclude the possibility that a third process explains both of them, and neither can it speak to the directional nature of the relationship. For example, increased arousal during successful stopping could lead to a phasic release of dopamine. The dopamine system influences GABA-ergic interneurons [37], which could result in reduced MEPs from M1. Such catecholamine release / arousal could also potentially lead to beta-band increases in the STN [38]. However, we find this explanation unlikely, as it predicts increased catecholamine release / arousal on failed stop-trials; yet beta-band power on such trials was significantly smaller compared to successful stop-trials, and the same was true for the amount of global CSE suppression (both of which is line with prior studies).

We found the association between the STN-LFP and CSE only for the right STN. This is in line with our previous fMRI study showed that right STN is engaged in stopping to a greater extent than left STN[12], as well as a meta-analytic search of the term "response inhibition" on neurosynth.org.

This study had some limitations. First, while we recorded LFP from the STN alone, similar beta band changes may occur in other basal ganglia nuclei [39]. Whether an increase in beta band power in other parts of the basal ganglia-thalamocortical circuit is related to stopping-induced changes in CSE associated will require further study. Ultimately, a strong demonstration that the STN is causally important for global motor suppression will require optogenetic or electrical stimulation, or measuring CSE during stopping in patients with STN lesions, c.f. [19]. Second, since these results were obtained from pathological brains, it cannot be assumed that these results apply to the healthy population. However, our PD patient sample showed increased activity in STN during stopping that are in line with fMRI

data from healthy participants[12]. Furthermore, the patients' MEP data showed the same stopping-related global reduction of motor excitability that is found in the healthy population[5-8]. Third, our sample size of nine patients is only modest. This reflects the difficulties in recruiting and performing the study in advanced Parkinson's disease patients who recently had deep brain stimulation surgery, and the considerable technical difficulty of simultaneously delivering TMS and recording LFP from the STN, moreover for a vocal stop-signal task for which TMS stimulation was time-locked to a real-time forecast of GoRT. Still, the sample size is similar to other studies of LFP during cognitive tasks. Moreover, we validated two well-established effects (global CSE suppression and successful- vs. failed-stop STN beta-band increase) in our sample prior to testing our main hypothesis. Additionally, our tests of the main hypothesis yielded a large effect size of d = 1.25 in the median split analysis, which was also confirmed as a single trial correlation with a group-level p-value of .011.

From a clinical perspective, our results have implications for the use of STN-DBS in PD. First, while STN-DBS *improves* motor performance in PD patients, it may *impair* functions that rely on global motor suppression. It has been proposed that perceptual or decision conflict recruit the STN, which ostensibly raises the decision threshold for multiple response channels (alternatively, this could be seen a suppression of activity of these channels[3, 27, 40, 41]). The consequence is to hold back all response tendencies, and buy time to accumulate more evidence about the correct action. STN-DBS has been shown to interfere with the normal ability to slow down responses in such high conflict conditions, so that patients instead responds more quickly / impulsively (i.e., they make more errors[40, 42, 43]). Our demonstration that global motor suppression is linked to STN activity provides more evidence for this model, which helps explain how and why STN DBS induces impulsivity. Second, beta oscillations have been proposed as a feedback signal for closed-loop DBS[44]. Our findings suggest that algorithms for closed-loop DBS should take into account changes in beta oscillations in a behavioral context. Third, by linking the STN signature with CSE, our results suggest that the CSE measure could potentially be used a proxy of STN function (at least in global suppression mode). This may be useful in future assessments of PD patients when STN-LFP recordings are not possible.

In summary, rapid action-stopping has global motor effects, and we show that these effects are related to beta-band activity within the STN. These results validate a core prediction of several basal ganglia models, which propose a broad suppressive impact of the STN on motor representations.

Acknowledgments

funding: This study was supported by the Canadian Institutes of Health Research (MOP15128), the National Institutes of Health (NS085543), and the James S McDonnell Foundation (220020375).

References

1. Bari A, Robbins TW. Inhibition and impulsivity: behavioral and neural basis of response control. Progress in neurobiology. 2013; 108:44–79. [PubMed: 23856628]
2. Aron AR, Robbins TW, Poldrack RA. Inhibition and the right inferior frontal cortex: one decade on. Trends Cogn Sci. 2014; 18(4):177–185. [PubMed: 24440116]

3. Zavala B, Zaghloul K, Brown P. The subthalamic nucleus, oscillations, and conflict. Movement disorders : official journal of the Movement Disorder Society. 2015; 30(3):328–338. [PubMed: 25688872]
4. Jahanshahi M, Obeso I, Baunez C, Alegre M, Krack P. Parkinson's disease, the subthalamic nucleus, inhibition, and impulsivity. Movement disorders : official journal of the Movement Disorder Society. 2015; 30(2):128–140. [PubMed: 25297382]
5. Badry R, Mima T, Aso T, et al. Suppression of human cortico-motoneuronal excitability during the Stop-signal task. Clin Neurophysiol. 2009; 120(9):1717–1723. [PubMed: 19683959]
6. Majid DS, Cai W, George JS, Verbruggen F, Aron AR. Transcranial magnetic stimulation reveals dissociable mechanisms for global versus selective corticomotor suppression underlying the stopping of action. Cereb Cortex. 2012; 22(2):363–371. [PubMed: 21666129]
7. Cai W, Oldenkamp CL, Aron AR. Stopping speech suppresses the task-irrelevant hand. Brain and language. 2012; 120(3):412–415. [PubMed: 22206872]
8. Wessel JR, Reynoso HS, Aron AR. Saccade suppression exerts global effects on the motor system. Journal of neurophysiology. 2013
9. Schmidt R, Leventhal DK, Mallet N, Chen F, Berke JD. Canceling actions involves a race between basal ganglia pathways. Nat Neurosci. 2013; 16(8):1118–1124. [PubMed: 23852117]
10. Isoda M, Hikosaka O. Role for subthalamic nucleus neurons in switching from automatic to controlled eye movement. The Journal of neuroscience : the official journal of the Society for Neuroscience. 2008; 28(28):7209–7218. [PubMed: 18614691]
11. Bastin J, Polosan M, Benis D, et al. Inhibitory control and error monitoring by human subthalamic neurons. Translational psychiatry. 2014; 4:e439. [PubMed: 25203170]
12. Aron AR, Poldrack RA. Cortical and subcortical contributions to Stop signal response inhibition: role of the subthalamic nucleus. The Journal of neuroscience : the official journal of the Society for Neuroscience. 2006; 26(9):2424–2433. [PubMed: 16510720]
13. Li CS, Huang C, Constable RT, Sinha R. Imaging response inhibition in a stop-signal task: neural correlates independent of signal monitoring and post-response processing. The Journal of neuroscience : the official journal of the Society for Neuroscience. 2006; 26(1):186–192. [PubMed: 16399686]
14. Kuhn AA, Williams D, Kupsch A, et al. Event-related beta desynchronization in human subthalamic nucleus correlates with motor performance. Brain : a journal of neurology. 2004; 127(Pt 4):735–746. [PubMed: 14960502]
15. Ray NJ, Brittain JS, Holland P, et al. The role of the subthalamic nucleus in response inhibition: evidence from local field potential recordings in the human subthalamic nucleus. Neuroimage. 2012; 60(1):271–278. [PubMed: 22209815]
16. Benis D, David O, Lachaux JP, et al. Subthalamic nucleus activity dissociates proactive and reactive inhibition in patients with Parkinson's disease. Neuroimage. 2014; 91:273–281. [PubMed: 24368260]
17. Siegel M, Donner TH, Engel AK. Spectral fingerprints of large-scale neuronal interactions. Nat Rev Neurosci. 2012; 13(2):121–134. [PubMed: 22233726]
18. Eagle DM, Bari A, Robbins TW. The neuropsychopharmacology of action inhibition: cross-species translation of the stop-signal and go/no-go tasks. Psychopharmacology. 2008; 199(3):439–456. [PubMed: 18542931]
19. Obeso I, Wilkinson L, Casabona E, et al. The subthalamic nucleus and inhibitory control: impact of subthalamotomy in Parkinson's disease. Brain : a journal of neurology. 2014; 137(Pt 5):1470–1480. [PubMed: 24657985]
20. Hazrati LN, Parent A. Convergence of subthalamic and striatal efferents at pallidal level in primates: an anterograde double-labeling study with biocytin and PHA-L. Brain Res. 1992; 569(2):336–340. [PubMed: 1371710]
21. Gillies AJ, Willshaw DJ. A massively connected subthalamic nucleus leads to the generation of widespread pulses. Proc Biol Sci. 1998; 265(1410):2101–2109. [PubMed: 9842737]
22. Nambu A, Tokuno H, Takada M. Functional significance of the cortico-subthalamo-pallidal 'hyperdirect' pathway. Neurosci Res. 2002; 43(2):111–117. [PubMed: 12067746]

23. Mink JW. The basal ganglia: focused selection and inhibition of competing motor programs. Progress in neurobiology. 1996; 50(4):381–425. [PubMed: 9004351]
24. Brainard DH. The Psychophysics Toolbox. Spatial vision. 1997; 10(4):433–436. [PubMed: 9176952]
25. Wessel JR, Aron AR. Unexpected events induce motor slowing via a brain mechanism for action-stopping with global suppressive effects. The Journal of neuroscience : the official journal of the Society for Neuroscience. 2013; 33(47):18481–18491. [PubMed: 24259571]
26. Verbruggen F, Logan GD. Models of response inhibition in the stop-signal and stop-change paradigms. Neurosci Biobehav Rev. 2009; 33(5):647–661. [PubMed: 18822313]
27. Wiecki TV, Frank MJ. A computational model of inhibitory control in frontal cortex and basal ganglia. Psychol Rev. 2013; 120(2):329–355. [PubMed: 23586447]
28. Parent A, Hazrati LN. Functional anatomy of the basal ganglia. II. The place of subthalamic nucleus and external pallidum in basal ganglia circuitry. Brain research Brain research reviews. 1995; 20(1):128–154. [PubMed: 7711765]
29. Frank MJ. Hold your horses: a dynamic computational role for the subthalamic nucleus in decision making. Neural networks : the official journal of the International Neural Network Society. 2006; 19(8):1120–1136. [PubMed: 16945502]
30. Keuken MC, Van Maanen L, Bogacz R, et al. The subthalamic nucleus during decision-making with multiple alternatives. Hum Brain Mapp. 2015; 36(10):4041–4052. [PubMed: 26178078]
31. Zavala BA, Tan H, Little S, et al. Midline Frontal Cortex Low-Frequency Activity Drives Subthalamic Nucleus Oscillations during Conflict. J Neurosci. 2014; 34(21):7322–7333. [PubMed: 24849364]
32. Brittain JS, Watkins KE, Joundi RA, et al. A role for the subthalamic nucleus in response inhibition during conflict. J Neurosci. 2012; 32(39):13396–13401. [PubMed: 23015430]
33. Greenhouse I, Sias A, Labruna L, Ivry RB. Nonspecific Inhibition of the Motor System during Response Preparation. J Neurosci. 2015; 35(30):10675–10684. [PubMed: 26224853]
34. Mansfield EL, Karayanidis F, Jamadar S, Heathcote A, Forstmann BU. Adjustments of response threshold during task switching: a model-based functional magnetic resonance imaging study. J Neurosci. 2011; 31(41):14688–14692. [PubMed: 21994385]
35. Siegert S, Herrojo Ruiz M, Brucke C, et al. Error signals in the subthalamic nucleus are related to post-error slowing in patients with Parkinson's disease. Cortex. 2014
36. Cavanagh JF, Sanguinetti JL, Allen JJ, Sherman SJ, Frank MJ. The Subthalamic Nucleus Contributes to Post-error Slowing. J Cogn Neurosci. 2014
37. Gorelova N, Seamans JK, Yang CR. Mechanisms of dopamine activation of fast-spiking interneurons that exert inhibition in rat prefrontal cortex. Journal of neurophysiology. 2002; 88(6): 3150–3166. [PubMed: 12466437]
38. Bockova M, Chladek J, Jurak P, Halamek J, Balaz M, Rektor I. Involvement of the subthalamic nucleus and globus pallidus internus in attention. J Neural Transm (Vienna). 2011; 118(8):1235–1245. [PubMed: 21191623]
39. Leventhal DK, Gage GJ, Schmidt R, Pettibone JR, Case AC, Berke JD. Basal ganglia beta oscillations accompany cue utilization. Neuron. 2012; 73(3):523–536. [PubMed: 22325204]
40. Frank MJ, Samanta J, Moustafa AA, Sherman SJ. Hold your horses: impulsivity, deep brain stimulation, and medication in parkinsonism. Science. 2007; 318(5854):1309–1312. [PubMed: 17962524]
41. Jahanshahi M, Obeso I, Rothwell JC, Obeso JA. A fronto-striato-subthalamic-pallidal network for goal-directed and habitual inhibition. Nat Rev Neurosci. 2015; 16(12):719–732. [PubMed: 26530468]
42. Zavala B, Damera S, Dong JW, Lungu C, Brown P, Zaghloul KA. Human Subthalamic Nucleus Theta and Beta Oscillations Entrain Neuronal Firing During Sensorimotor Conflict. Cereb Cortex. 2015
43. Wylie SA, Ridderinkhof KR, Elias WJ, et al. Subthalamic nucleus stimulation influences expression and suppression of impulsive behaviour in Parkinson's disease. Brain : a journal of neurology. 2010; 133(Pt 12):3611–3624. [PubMed: 20861152]

44. Little S, Beudel M, Zrinzo L, et al. Bilateral adaptive deep brain stimulation is effective in Parkinson's disease. J Neurol Neurosurg Psychiatry. 2015

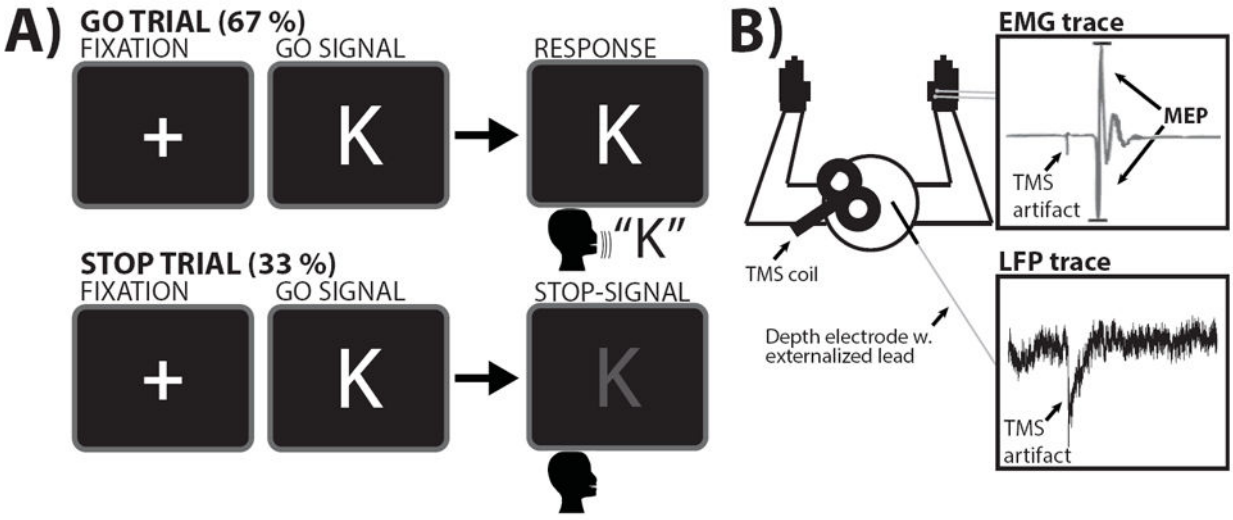

Figure 1.

A) SST task diagram. Note that the stop-signal consisted of the letter turning from white to red. B) LFP and EMG recordings. Participants performed a verbal stop-signal task while MEPs were recorded from the right hand, which was resting and not involved in the task. Furthermore, LFP data was simultaneously collected from the externalized STN electrode lead.

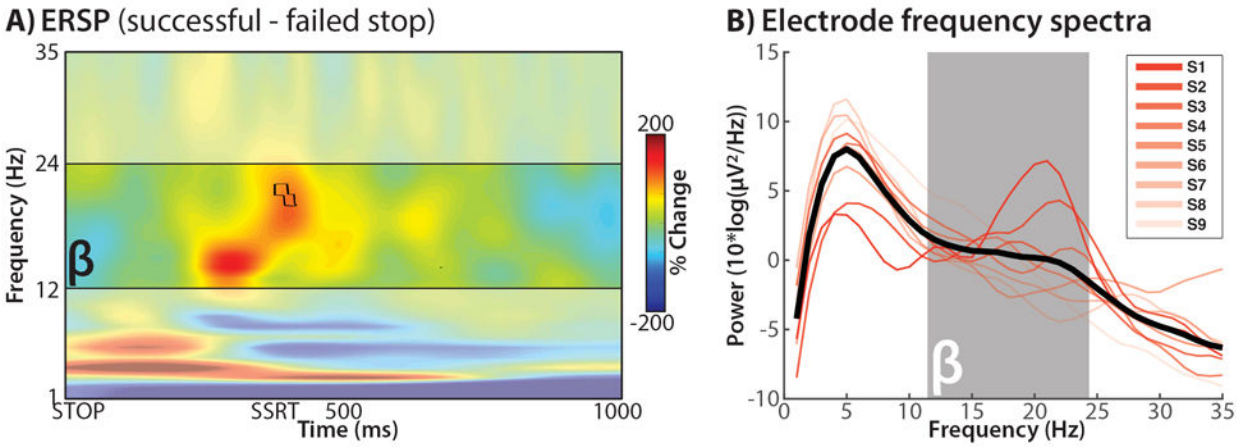

Figure 2.

A) Full spectrum ERSP data from the LFP-only phase (no TMS; the bipolar STN channels underlying this figure were selected from the simultaneous LFP-TMS data to perform the main analysis in Figure 3). Depicted is the difference between successful and failed stop trials, time-locked to the stop-signal (STOP); red: successful > failed, blue: failed > successful. Black outline: $p < .00417$. B) Individual channel power spectra for each selected channel. Note the uptick in beta power in each individual channel.

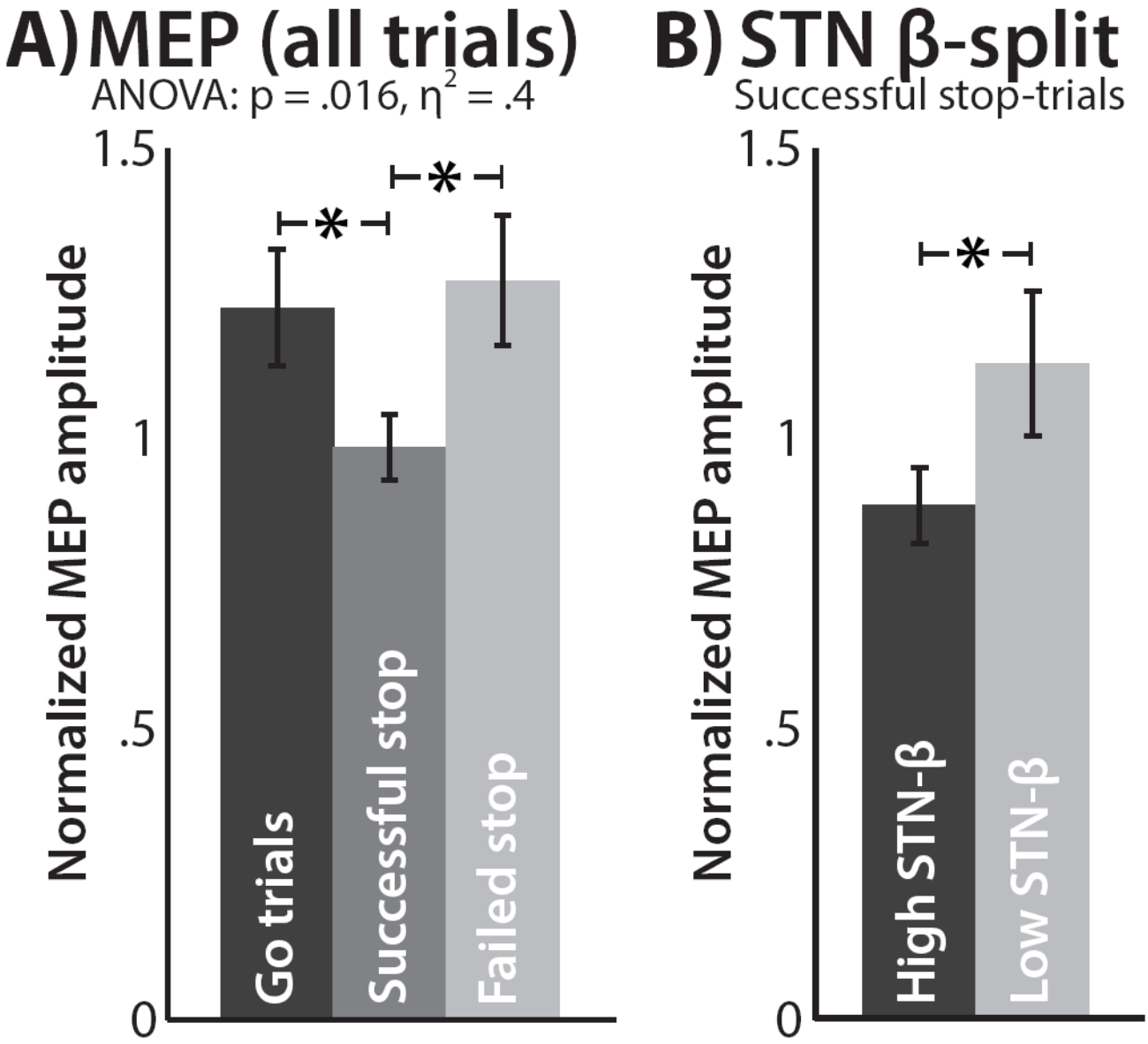

Figure 3.

FDI-MEP from the simultaneous LFP-TMS phase. A) FDI-MEP results, split by trial type, normalized by inter-trial baseline. B) FDI-MEP results for successful stop-trials, split by pre-pulse beta-band amplitude. Error bars represent the standard error of the mean.

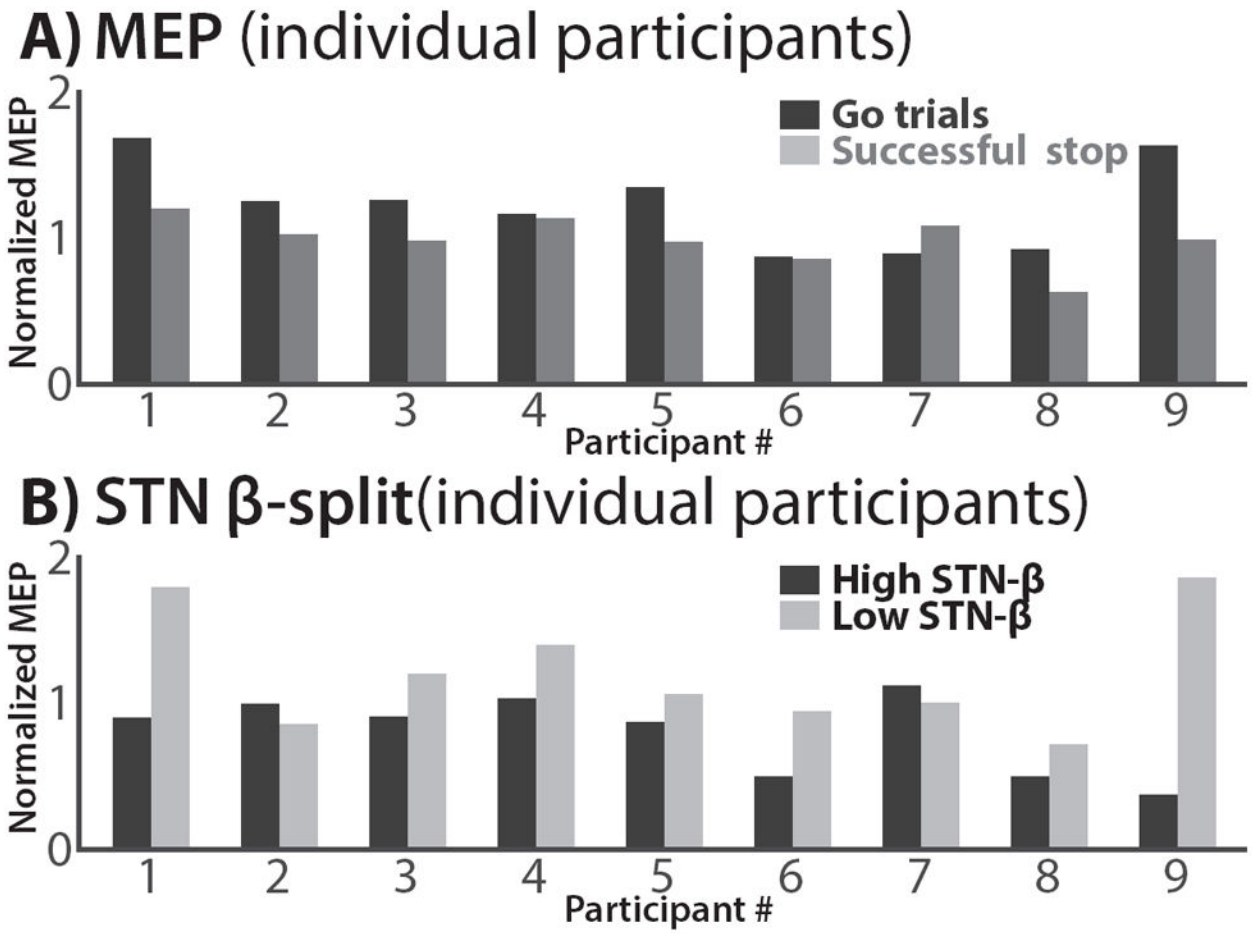

Figure 4.

FDI-MEP from the simultaneous LFP-TMS phase; individual subjects. A) All but one subject show FDI-MEP suppression for successful stop trials vs. go trials. B) All but two subjects show greater FDI-MEP suppression for successful stop-trials with greater beta-power.

Table 1

Behavioral data from the two phases of the experiment.

Variable	LFP-only	LFP-TMS	p
GoRT	678	702	0.37
FsRT	603	621	0.35
p(stop)	0.54	0.53	0.9
SSD	304	363	0.19
SSRT	374	338	0.32

Left column: LFP-only phase, right column: simultaneous LFP-TMS phase. P-values denote significance of a two-sided paired samples t-test for differences between the two phases. GoRT = go reaction time. FsRT = Failed stop-trial reaction time. P(stop) = probability of successful stopping. SSD = stop-signal delay. SSRT = stop-signal reaction time.